International Journal of Greenhouse Gas Control 6 (2012) 21–36

Contents lists available at SciVerse ScienceDirect

International Journal of Greenhouse Gas Control

journal homepage: www.elsevier.com/locate/ijggc

A rate based model of a packed column for CO_2 absorption using aqueous monoethanolamine solution

Patricia Mores[a], Nicolas Scenna[a,b,1], Sergio Mussati[a,b,*]

[a] UTN–FRRo, Zeballos 1341, S2000BQA, Rosario, Argentina
[b] INGAR/CONICET, Instituto de Desarrollo y Diseño, Avellaneda 3657, 3000 Santa Fe, Argentina

ARTICLE INFO

Article history:
Received 4 May 2011
Received in revised form
16 September 2011
Accepted 29 October 2011
Available online 30 December 2011

Keywords:
Post-combustion CO_2 capture
Rate based models
CO_2 reactive absorption into amine solutions
Absorber mathematical model
Simulation
Optimization

ABSTRACT

A comprehensive and simplified rate based mathematical model of a packed column for CO_2 capture using aqueous monoethanolamine (MEA) solution is developed. The absorption unit model takes into account the effect of kinetic reactions on the mass transfer, the thermodynamic non-idealities, the hydraulics of the random packing and the absorber dimensions (diameter and height). It is implemented into the optimization environment GAMS (General Algebraic Modeling System).

The proposed NLP model was validated by comparison of obtained results with published experimental data. Good accuracy of results has been obtained for experimental pilot plant scales. Once validated, the model was used to investigate the influence of main process parameters and the effect of different correlations to compute the effective interfacial area for mass transfer (a/a_t) on the absorption efficiency. Obtained results indicate that model solutions depend strongly on the correlations used to compute the (a/a_t). In addition, results assuming thermal equilibrium and thermal non-equilibrium in liquid and vapor phases were also compared. For both conditions and specific cases, similar concentration and temperature profiles in the liquid phase in the absorber were obtained.

Finally, results obtained by solving different optimization problems are discussed. More precisely, the optimization consisted in determining the operating conditions to maximize the absorption efficiency defined as the ratio between the CO_2 recovery in rich solution and the packing volume of the column. The effect of the main process parameters on the optimized results was also investigated.

1. Introduction

Many specialists predict for next decades that the coal and natural gas will dominate the electricity generation. Precisely, predictions indicate that coal is abundantly available to be used as a primary source of energy for next 160 years, approximately three times that of natural gas. Therefore, the reduction of CO_2 emissions is a global challenge and requires collective actions and close cooperation between industries and researchers.

Carbon dioxide capture and storage (CCS) is widely recognized as a viable technology option for the mitigation of greenhouse gas emissions from large sources.

Specifically, in the electricity and heat sector, the options to capture CO_2 from exhaust flue gas generated depends on the fossil fuel used and on the conditions of the flue-gas to be treated (CO_2 concentration and pressure). The following are the three main technologies that have been proposed for the capture of carbon dioxide: (1) pre-combustion capture, (2) oxi-fuel combustion capture and (3) post-combustion CO_2 capture.

In this paper, the amine-based CO_2 capture from flue-gas is particularly studied. This technology is especially well-suited for retrofitting existing power plants because it does not require significant changes in the equipment configuration. It is, however, in its infancy and is several years away from commercial development. The main challenges are the improvement of the operating and investment costs and efficiency as well.

Process modeling and mathematical programming techniques have emerged as important tools to study and to analyze any chemical/industrial processes in detail. Certainly, realistic process models are becoming almost indispensable for optimal synthesis and design of processes because they provide guidance on the development of novel and feasible processes.

Typically, reactive absorption units have been modeled and simulated assuming well-known equilibrium stage model and the resulting mathematical model is then solved using iterative and trial-error procedures. Thus, the absorber is subdivided into height stages using height equivalent to a theoretical plate (HETP)

* Corresponding author. Tel.: +54 342 4534451; fax: +54 342 4553439.
E-mail addresses: patricia_mores@hotmail.com (P. Mores), nscenna@santafe-conicet.gov.ar (N. Scenna), mussati@santafe-conicet.gov.ar (S. Mussati).
[1] Tel.: +54 342 4534451; fax: +54 342 4553439.

1750-5836/$ – see front matter © 2011 Elsevier Ltd. All rights reserved.
doi:10.1016/j.ijggc.2011.10.012

Nomenclature

A	cross-sectional area of column (m^2)
a_t	specific dry area of packing (m^2/m^3)
a	effective mass transfer area (m^2/m^3)
$D^L_{CO_2}$	CO_2 diffusivity (m^2/s)
D^G	gas diffusivity (m^2/s)
D_p	nominal packing size (m)
E	enhancement factor
F_p	packing factor
EM	equilibrium model
g	gravitational constant (m/s^2)
h	stage height (m)
H^L	liquid enthalpy (kJ)
H^G	gas enthalpy (kJ)
ΔH_R	reaction heat (kJ)
$\Delta \dot{H}_R$	specific reaction heat (kJ/mol CO_2)
ΔH_{H_2O}	vaporization heat of water (kJ)
$\Delta \dot{H}_{H_2O}$	specific vaporization heat of water (kJ/mol H_2O)
H_{CO_2}	CO_2 solubility in MEA–H_2O solution (kPa)
H_{CO_2-MEA}	CO_2 solubility in MEA (Pa/m^3 mol)
$H_{CO_2-H_2O}$	CO_2 solubility in H_2O (Pa/m^3 mol)
HTU	height of a transfer unit (m)
K_m	equilibrium constant of reaction
k_r	forward reaction constant (mol/m^3)
k^L	liquid-side mass transfer coefficient (m/s)
k^G	gas-side mass transfer coefficient (kmol/Pa s m^2)
L	liquid flow-rate (mol/s)
L'	liquid mass velocity (kg/s m^2)
G	gas flow-rate (mol/s)
G'	gas mass velocity (kg/s m^2)
M^L	liquid molecular weight
MEA	monoethanolamine
NTU	Number of transfer units
P	pressure (kPa)
pH_2O	partial pressure of water (kPa)
ΔP_d	dry pressure drop (kPa/m)
ΔP_L	pressure drop due to liquid presence (kPa/m)
ΔP	total pressure drop (kPa)
R	universal gas constant
RBM	rate based model
T	temperature (K)
u_f	flooding velocity (m/s)
u_{sg}	superficial gas velocity (m/s)
x	liquid mole fraction
y	gas mole fraction

Greek symbols

γ	activity coefficient
φ	fugacity coefficient
α	CO_2 loading
μ^L	liquid viscosity (kg/m s)
μ^G	gas viscosity (kg/m s)
ρ'^L	mass liquid density (kg/m^3)
ρ'^G	gas mass density (kg/m^3)
ρ^G	molar gas density ($kmol/m^3$)
η	Murphree's efficiency
σ	surface tension (N/m)
σ_C	packing surface tension (N/m)
ψ	Ion charge
λ	stripping factor

Superscripts

L	liquid phase
G	gas phase
0	initial

Subscripts

z	stage
$z+1$	stage above z
$z-1$	stage below z
j	gas component
i	liquid component
m	reaction

and is assumed the equilibrium state (mechanical, thermal and chemical equilibria) between the liquid and vapor leaving the stage (Taylor and Krishna, 1993). However, equilibrium is rarely attained at a stage since absorption is a rate controlled phenomenon (Chakravarty et al., 1985). Equilibrium models may be inadequate when mass and heat transfer are kinetically limited processes driven by gradients of the chemical potential and temperature (Kucka et al., 2003). Thus, a better estimation is provided by the rate-based approach. Thus, the influence of the chemical reaction on mass transfer can be accounted for by enhancement factors in a simple way. Enhancement factors can be found in the literature for different types of reactions, reaction orders and reaction pathways based on the film theory, penetration theory or surface renewal theory. They are either derived analytically by solving the governing differential equations with a reaction rate term in the film or approximate solutions are given. For complex reaction systems no reliable enhancement factors might be available. In these cases a typical approach is to divide the film in radial segments. The reactions are then incorporated by adding reaction rate terms into the component balances for each film segment. This approach has the highest complexity, does not require enhancement factors and can handle many different reactions. However, the computational effort compared to the enhancement factor approach rises significantly, since all equations for mass and heat transport, chemical reactions and thermodynamic properties have to be computed for each film element. The resulting model size depends on the number of film elements. It is usually between 6 and 40 for an accurate calculation of the film profiles (Asprion, 2006). According to this, different rate based models may be derived depending on the assumptions and approximations used.

Currently, research effort is also being devoted to the overall reaction mechanisms involved in the CO_2 absorption into amine and its effects on the absorption efficiency (Sexton and Rochelle, 2011; Bedell, 2011; Qin et al., 2010; Mindrup and Schneider, 2010; Lepaumier et al., 2009a,b; Lepaumier et al., 2010). In addition, detailed mathematical models based on both film and penetration theories are being developed (Simon et al., 2011; Faramarzi et al., 2010; Edali et al., 2009; Zhang et al., 2009; Lawal et al., 2009; van Loo et al., 2007).

This paper presents a comprehensive and simplified rate based mathematical model for a packed column for the reactive absorption of CO_2 into aqueous amine solution. The mathematical model to be presented in this work is the first basic step of a more ambitious project aimed at determining the optimal synthesis and design of electricity power plant including the capture of the CO_2 due to the fuel combustion.

An aqueous MEA solution is specifically considered for the CO_2 capture. The proposed model is deterministic and includes process-specific data related to reaction kinetics, diffusivities, solubility, thermodynamic equilibrium data, viscosity and densities. The influence of the main model parameters as well as the performance of different correlations used to compute the effective

interfacial area for mass transfer on the CO_2 absorption efficiency are investigated. In addition, the absorber dimensions such as packing height and absorber diameter are considered as optimization variables. Moreover, results obtained by assuming thermal equilibrium and non-equilibrium are compared.

GAMS (General Algebraic Modeling System) which is a high-level algebraic modeling system for large scale optimization is used for implementation and solving the resulting mathematical model. In general, mathematical programming environments such as GAMS, have shown to be powerful tools, specially when the optimization problem is large, combinatorial and highly non-linear.

The model is flexible enough to be used for simulation and optimization purposes, depending on the degree of freedom of the mathematical model. For instance, the user can fix the degree of freedom in order to simulate the absorber. In contrast to this, if the degree of freedom is different from zero, the user can formulate different optimization problems by selecting different objective functions. Optimal dimensions and temperature, concentration and flow-rate profiles are obtained as model results. Here, simulated and optimized results are presented and discussed in detail.

The paper is outlined as follows. Section 2 introduces the problem formulation. Section 3 lists the assumptions and the mathematical model. Section 4 presents applications of the developed NLP model. Obtained results are discussed in Section 5. Finally, Section 6 presents the conclusions and future work.

2. Problem statement

The proposed optimization problem can be stated as follows. Given the flue-gas conditions (composition, temperature and flow-rate), the goal is to determine the optimal operating conditions in order to maximize the ratio between the CO_2 recovery in rich solution and packing volume.

Optimal temperature, composition and flow-rates profiles along the absorber are simultaneously obtained. Exploiting the robustness and flexibility of the proposed model, the influence of the main process parameters (absorber dimensions, amine solution temperature and CO_2 recovery in rich solution, CO_2 removed from the flue-gas stream and L/G ratio, among others) on the absorption performance is also investigated.

3. Assumptions and mathematical model

Fig. 1 schematically shows a non-equilibrium stage "z" used to model the absorber. In this figure, z ($z = 1, \ldots, N$), j ($j = CO_2, N_2, H_2O$, and O_2) and i ($i = CO_2$, MEA, H_2O, $MEAH^+$, $MEACOO^-$, HCO_3^-, CO_3^{2-}, H_3O^+, and HO^-) denote each stage and either gas and liquid component, respectively. As shown, the vapor goes up into stage z from stage $z-1$ and the liquid flows down into stage z from stage $z+1$.

The main model assumptions can be summarized as follows:

- The total height of absorber column is divided into N stages which allow to compute profiles of temperatures, flow-rates and compositions along the column. Ten stages ($N = 10$) are considered in this paper.
- Liquid and vapor phases are well-mixed. Thus, there is no concentration and temperature gradients in single liquid and vapor phases and point efficiency is equivalent to Murphree's efficiency (η).
- Stage efficiency may be computed similarly to the tray efficiency. Dependence of stage efficiency with gas and liquid velocities and enhancement factor, among others, is considered.

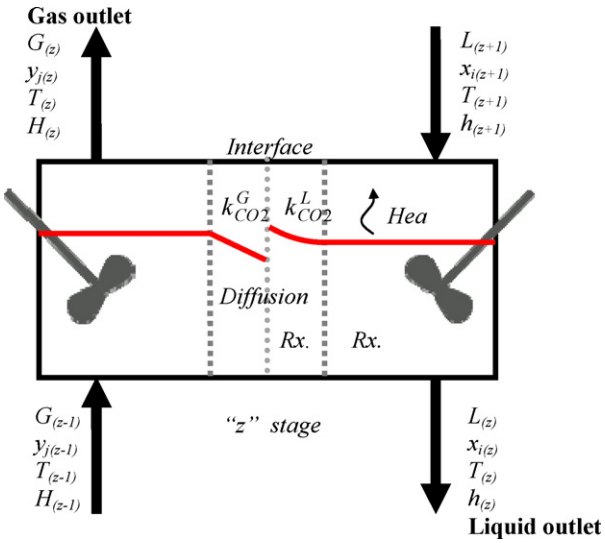

Fig. 1. Non equilibrium stage "z".

- Non-ideal behavior in the gas phase is assumed. Fugacity coefficients are computed by using Peng–Robinson equations of state for a multi-component mixture (Peng and Robinson, 1976).
- As first approximation, ideal behavior in the liquid phase is assumed.
- An enhancement factor is used to introduce the effect of the chemical reaction on the CO_2 transfer.
- Aqueous MEA amine solution is used as the solvent (30 wt.%).
- As first approximation, thermal equilibrium is assumed between the liquid and gas phases.
- Pressure drop along the absorber is considered.
- Absorber dimensions (height and diameter) are considered as optimization variables. Thus, this assumption allows simultaneous optimization of the size of the column and the operating conditions.
- CO_2 and H_2O are the only species transferred across the interface. This assumption is widely accepted in the literature (deMontigny et al., 2006).
- Dependence of liquid and vapor enthalpies with the temperature and composition are considered.
- Dependence of aqueous alkanolamine solution density with the temperature is taken into account.
- Dependence of transfer coefficient in liquid and vapor phases with the viscosity, density, nominal packing size and specific dry area and effective interfacial area for mass transfer are taken into account.
- An upper bound (1.225 kPa/m of packing) for the maximum allowable pressure drop is considered (Kister, 1992). Thus, the total pressure drop may be lower than the upper bound.
- Lower and upper bounds for the superficial gas velocity are also considered to avoid flooding problem and a bad gas–liquid distribution. Values suggested in literature range from 60 to 80% of the flooding velocity.
- It is assumed that absorber diameter should be ten times greater than the nominal diameter of packing. A maximum absorber diameter is adopted (13.5 m). This upper bound is suggested in the literature (Kister, 1992; Perry and Green, 1997; Mccabe et al., 2005).
- A low CO_2 concentration in flue gas stream is assumed to study the accuracy of the proposed model and previous assumptions. The main reason of this is that the developed model will be coupled into a combined cycle power plant in order to optimize the

whole integrated plant. The CO_2 concentration in exhaust gases of such power plants is low.

- Chemical reactions take place at the liquid and vapor interface. The following reactions are considered:

$$2H_2O \leftrightarrow H_3O^+ + OH^- \quad (R1)$$

$$2H_2O + CO_2 \leftrightarrow H_3O^+ + HCO_3^- \quad (R2)$$

$$H_2O + HCO_3^- \leftrightarrow H_3O^+ + CO_3^{2-} \quad (R3)$$

$$H_2O + MEAH^+ \leftrightarrow H_3O^+ + MEA \quad (R4)$$

$$MEACOO^- + H_2O \leftrightarrow MEA + HCO_3^- \quad (R5)$$

$$MEA + CO_2 + H_2O \leftrightarrow MEACOO^- + H_3O^+ \quad (R6)$$

$$CO_2 + OH^- \leftrightarrow HCO_3^- \quad (R7)$$

By considering all listed hypothesis the following rate based model was derived.

3.1. Overall mass and energy balances in stage "z"

$$L_{z+1} - L_z + G_{z-1} - G_z = 0 \quad (1)$$

$$L_{z+1}H^L_{z+1} - L_z H^L_z + G_{z-1}H^G_{z-1} - G_z H^G_z + (\Delta H_R)_z - (\Delta H_{H_2O})_z = 0 \quad (2)$$

where L, G, H^L and H^G refer to the liquid and vapor flow-rates and enthalpies respectively. ΔH_R and ΔH_{H_2O} are the heat released by the reaction and vaporization heat of water and the corresponding correlations are taken from Oyenekan (2007) and Hilliard (2008).

3.2. Species mass balance in stage "j"

$$L_{z+1}x_{iz+1} - L_z x_{iz} + G_{z-1}y_{jz-1} - G_z y_{jz} = 0 \quad (3)$$

x_i and y_j refer to the mole fraction of component "i" or "j" in liquid and vapor phases respectively.

$$\sum y_{jz} = 1 \quad j = CO_2, H_2O, N_2, O_2 \quad (4)$$

$$\sum x_{iz} = 1 \quad i = CO_2, H_2O, MEA, MEAH^+, MEACOO^-, H_3O^+, HO^-, HCO_3^-, CO_3^{2-} \quad (5)$$

3.3. Chemical reactions and phase equilibrium relationship

The dependences of the equilibrium constants K_m of reactions R_1–R_5 and Henry's coefficient ($H_{CO_2,i,z}$) with the temperature are computed as follows:

$$(K_m)_z = \prod_i (a_{iz})^{\nu_i} = \prod_i (x_{iz}\gamma_{iz})^{\nu_i} \quad \forall m, \quad m = R_1, R_2, R_3, R_4, R_5 \quad (6)$$

$$(K_m)_z = \exp\left(A + \left(\frac{B}{T_z}\right) + C\ \ln(T_z)\right) \quad \forall m, \quad m = R_1, R_2, R_3, R_4, R_5 \quad (7)$$

$$H_{CO_2,i,z} = \exp\left(A + \left(\frac{B}{T_z}\right) + C\ \ln(T_z) + DT_z\right) \quad \forall i, \quad i = MEA, H_2O \quad (8)$$

T refers to the absolute temperature (K) and a_{iz}, γ_{iz}, ν_i are, respectively, activity, activity coefficient and stoichiometric coefficient for component "i" in reaction "m" at stage "z". Liquid phase has ideal behavior, therefore the activity coefficients are set to one (Kent–Eisenberg model).

$$y_{CO_2 z}\varphi_{CO_2 z}P_z = H_{CO_2 z}[CO_2]_z \quad (9)$$

$$y_{H_2O z}\varphi_{H_2O z}P_z = p_{H_2O z}x_{H_2O z} \quad (10)$$

where $[i]_z$ is the molar concentration of specie "i" in stage "z". φ_z, P_z and $p_{H_2O\,z}$ refer to fugacity coefficient, total pressure and partial pressure of water, respectively.

Solubility of CO_2 in MEA solution (H_{CO_2}), which is corrected for solution ionic strength (I), is calculated as follow (Greer, 2008):

$$H_{CO_2\ z} = (10^{0.152 I_z})\left[\frac{(x_{H_2O z}H_{CO_2\,MEA\,z} + x_{CO_2\ z}H_{CO_2\,H_2O\,z})}{\rho^L_z}\right] \quad (11)$$

$$I_z = \frac{1}{2}\sum_i \psi_i[i]_z \quad \forall\ i, \quad i = MEAH^+, MEACOO^-, H_3O^+, OH^-, CO_3^{2-}, HCO_3^- \quad (12)$$

where ψ_i is the ion charge.

Values of the coefficients used in Eqs. (7) and (8) are listed in Table 1. Antoine equation is used to predict the partial vapor pressure of water (p_{H_2O}).

3.4. Ionic mass balance relationship in stage "z"

$$[MEAH^+]_z + [H_3O^+]_z = [MEACOO^-]_z + [HCO_3^-]_z + 2[CO_3^{2-}]_z + [OH^-]_z \quad (13)$$

$$\alpha[MEA]^0_z = [CO_2]_z + [MEACOO^-]_z + [HCO_3^-]_z + [CO_3^{2-}]_z \quad (14)$$

$$[MEA]^0_z = [MEA]_z + [MEAH^+]_z + [MEACOO^-]_z \quad (15)$$

The superscript (0) refers to the initial condition. CO_2 loading (α) is defined as the ratio between total CO_2 and total amine.

3.5. Enhancement factor

The influence of the reactions on the CO_2 transfer is considered by an enhancement factor (E) which is defined as follows:

$$E_z = \frac{\sqrt{(D^L_{CO_2})_z[(k_{r,CO_2-MEA})_z[MEA]_z + (k_{r,CO_2-OH})_z[CO_2]_z]}}{k^L_z} \quad (16)$$

The forward constants ($k_{r,\,CO_2-MEA}$ and $k_{r,\,CO_2-OH}$) of the parallel and kinetically controlled reactions (R6) and (R7) are taken from Kucka et al. (2002) and Aboudheir et al. (2003) and are computed as follows:

$$(k_{r,CO_2-MEA})_z = 4.495 \times 10^{11} \quad \exp\left(-\frac{44,940}{RT_z}\right) \quad (17)$$

$$(k_{r,CO_2-OH})_z = \exp\left(31.396 - \frac{6658}{T_z}\right) \quad (18)$$

The constraints used to compute CO_2 diffusivity ($D^L_{CO_2}$) and liquid-side mass transfer coefficient (k^L_z) are taken from Greer (2008) and Onda et al. (1968), respectively. They depend on the viscosity and mass density, the nominal packing size, specific dry area and the effective interfacial area for mass transfer.

Table 1
Parameters of chemical reactions and Henry's coefficient.

	A	B	C	D	Reference
K_1	140.932	−13445.9	−22.4773	0	Aboudheir et al. (2003)
K_2	235.482	−12,092	−36.7816	0	Aboudheir et al. (2003)
K_3	220.067	−12431.7	−35.4819	0	Aboudheir et al. (2003)
K_4	6.69425	−3090.83	0	0	Aboudheir et al. (2003)
K_5	−3.3636	−5851.11	0	0	Aboudheir et al. (2003)
HCO_2–H_2O	170.7126	−8477.771	−21.95743	0.005871	Liu et al. (1999)
HCO_2–MEA	89.451	−2934.6	−11.592	0.016440	Liu et al. (1999)

3.6. Effective interfacial area of packing for mass transfer

The effective mass transfer area (m^2/m^3) is considered as an optimization variable which depends, among others, on the cross-sectional area of column, liquid flow-rate, density, viscosity and superficial tension.A number of correlations exist for calculating the effective interfacial area for mass transfer. In this work, the proposed model will be solved for three correlations in order to study the effect of such correlations on the optimal solutions. Precisely, the following correlations are considered:

- Correlation proposed by Onda et al. (1968):

$$a_z = a_t \left(1 - \exp\left(-1.45\left(\frac{\sigma_c}{\sigma_z}\right)^{0.75}\left(\frac{L'_z}{a_t\mu_z^L}\right)^{0.1}\left(\frac{(L'_z)^2 a_t}{(\rho'^L_z)^2 g}\right)^{-0.05}\left(\frac{(L'_z)^2}{\rho'^L_z \sigma_z a_t}\right)^{0.2}\right)\right) \quad (19.a)$$

- Correlation proposed by Wilson (2004):

$$a_z = \exp(4.73)(u_z^G)^{0.061}\left(\frac{L_z M_z^L}{1000 A_z}\right)^{0.148} \quad (19.b)$$

- Correlation proposed by Bravo and Fair (1982):

$$a_z = a_t\ 0.310\frac{\sigma_z^{0.5}}{h_z^{0.4}}\left(\left(\frac{\mu_z^L L'_z}{\rho'^L_z \sigma_z^L}\right)\left(\frac{6G'_z}{a_t\mu_z^G}\right)\right)^{0.392} \quad (19.c)$$

where A, σ, σ_c, u^G, M^L and h are cross-sectional area of column, liquid surface tension, surface tension of packing material, superficial gas velocity, liquid molecular weight and stage height, respectively.

3.7. Pressure drop

The following correlation computes the total pressure drop along the stage "z".

$$\Delta P_z = (\Delta P_d)_z + (\Delta P_L)_z \quad (20)$$

where $(\Delta P_d)_z$ and $(\Delta P_L)_z$ refer, respectively, to the dry pressure drop and pressure drop due to the liquid presence and depend on the gas and liquid loading factors.

Finally, the total pressure drop along the absorber is given by:

$$\Delta P = \sum_z \Delta P_z h_z \quad (21)$$

3.8. Dependence of the stage efficiency with the absorber height and process variables

According to the third hypothesis, the stage efficiency can be computed as:

$$\eta_z = 1 - \exp\left(-\frac{HTU_z}{h_z}\right) = 1 - \exp\left\{-\frac{[((G'_z)/(RT_z a_z k_z^G \rho'^G_z))] + \lambda_z[((L'_z)/k_z^L a_z \rho'^L_z E_z)]}{h_z}\right\} \quad (22)$$

where

$$h_z = HTU_z \times NTU_z \quad (23)$$

NTU_z and HTU_z are the number of transfer units based in the total mass transfer coefficient and the transfer unit height, respectively. G' and L' are gas and liquid mass velocities (kg/m^2 s), ρ'^G and ρ'^L are gas and liquid mass densities (kg/m^3); λ is the stripping factor ($\lambda = m/(L/G)$), and k^G is the gas-side mass transfer coefficient (kmol/Pa s m^2).

Finally, as mentioned earlier, h, a, k^L and E are the height of the stage (m), effective interfacial area for mass transfer (m^2/m^3), liquid-side mass transfer coefficient (m/s) and dimensionless enhancement factor, respectively.

3.9. Dimensions

The diameter of each stage (DT_z) is computed as follows:

$$DT_z = \sqrt{\frac{4\,G_z}{u_{sg,z}\pi\rho_z^G}} \quad (24)$$

where ρ^G, G and $u_{sg,z}$ refer to the gas density, flow-rate and superficial velocity respectively. Then, $u_{sg,z}$ is related to the flooding velocity [u_{fz}] by Eq. (25)

$$u_{sg,z} = f_z u_{fz} \quad (25)$$

where f_z ranges from 0.6 to 0.8 (lower and upper bounds).

In order to consider a same diameter in all stages, the following constraint should be imposed:

$$DT_z = DT_{z+1} \quad z = 1, \ldots, 9 \quad (26)$$

3.10. Total packing volume

The packing volume is an optimization variable and depends on the cross-sectional area and height of column. It is computed by the following constraint:

$$\text{Packing volume} = \sum_{z=1}^{N} \pi \cdot \left(\frac{DT_z}{2}\right)^2 \cdot h_z \quad (27)$$

3.11. CO_2 removed from the flue-gas

The CO_2 captured form the flue-gas (%) is computed as follows:

$$CO_2 \text{ removed from the flue gas} = \frac{G^{in} y_{CO_2}^{in} - G^{out} y_{CO_2}^{out}}{G^{in} y_{CO_2}^{in}} \quad (28)$$

where G^{in} and $y_{CO_2}^{in}$ refer to the inlet gas flow-rate and composition and are fixed and known values (model parameters). G^{out} and $y_{CO_2}^{out}$ refer to the outlet gas flow-rate and composition and are model variables.

3.12. CO_2 recovery in rich solution (%)

The following constraint is used to compute the percentage of the CO_2 recovery in rich solution:

$$CO_2 \text{ recovery in rich solution} = \left[\frac{L^{out}x^{out}_{CO_2}}{G^{in}y^{in}_{CO_2} + L^{in}x^{in}_{CO_2}}\right] \quad (29)$$

where L and x refer to the liquid flow-rate and composition, respectively.

3.13. Objective function

An objective function defined as the ratio between the CO_2 recovery in rich solution and the total packing volume is proposed (maximization):

$$OF = \left[\frac{CO_2 \text{ recovery in rich solution}}{\text{Total packing volume}}\right] \quad (30)$$

The model also includes constraints to compute the enthalpies, fugacity coefficients and surface tension, among others, which can be found elsewhere (Austgen, 1989; Freguia, 2002; Dugas, 2006; Greer, 2008).

Thus, Eqs. (1)–(30) are basically the main constraints used to describe and optimize the steady state absorption process. The optimization model, which is referred to by the abbreviation RBM, involves approximately 1500 variables and constraints. It was implemented in General Algebraic Modeling System (GAMS) (Brooke et al., 1996). The generalized reduced gradient algorithm CONOPT 2.041 was here used as NLP solver (Drud, 1992).

It should be noticed that global optimal solutions cannot be guaranteed due to some non-convex constraints involved in some of the mathematical model (bilinear terms, logarithms, and among others).

The equilibrium model, which is used later for comparison purposes and will be referred to by the abbreviation EM, was derived from the model presented above. Basically, it involves Eqs. (1)–(15) plus the following constraint used to compute the Murphree's stage efficiency in each stage (η_z):

$$\eta_z = \frac{G_z y_{CO_2,z} - G_{z-1} y_{CO_2,z-1}}{G_z y^*_{CO_2,z} - G_{z-1} y_{CO_2,z-1}}$$

where $y^*_{CO_2,z}$ refers to the equilibrium CO_2 composition in the gas phase leaving the stage "z".

Two values for η_z are considered in this paper (30% and 40%). Thus, the output results obtained by the RBM using different correlations for calculating the effective interfacial area for mass transfer and EM using two values for η_z are compared.

4. Results: application of the NLP model

In this section, two examples are presented in order to validate the proposed model (Example 1) and to discuss the optimization results (Example 2).

Intel Core 2 Quad Extreme QX9650 3 GHz 1333 MHz processor and 4 GB RAM has been used to perform the simulations and optimizations.

4.1. Example 1: model validation

The model validation was performed for different flue-gas flow-rates by comparing the predicted results with experimental data. Pilot plant's data reported by Tontiwachwuthikul et al. (1992) and by Alatiqi et al. (1994) were used to validate the model output results for low and medium flue-gas flow-rates, respectively. Only for validation purpose, both models (EM and RBM) were used as a simulators in a predictive manner, that is, no parameters were fitted to the experimental data.

Table 2
Parameter values of flue-gas conditions (Tontiwachwuthikul et al., 1992).

	Flue-gas	Lean amine
Temperature (K)	288.15	292.15
Total flow-rate (mol/s)	0.14	1.03
H_2O (mole fraction)	0.10	0.94
CO_2 (mole fraction)	0.19	0.00
MEA (mole fraction)	0.00	0.06
N_2 (mole fraction)	0.71	0.00
Pressure (kPa)	101.3	101.3

Table 3
Parameter values of absorber and packing specifications.

Column type	Packed
Diameter (m)	0.10
Total packing height (m)	6.55
Stages number	10
Packing specifications	
Type of packed	Ceramic berl saddles
Specific interfacial area (m^2/m^3)	545
Nominal packing size (m)	0.013
Surface tension (N/m)	0.061

4.1.1. Model validation at low flue-gas flow-rate

Tables 2 and 3 summarize the model parameter values corresponding to the absorber column and packing specifications used for validation.

Figs. 2–5 compare the predicted and experimental data in terms of the CO_2 mole fraction, CO_2 loading (α) defined as the ratio between CO_2 mol and MEA mol in the amine solution and liquid temperature profiles along the absorber. Results obtained using process simulator HYSYS are also illustrated because it is widely used by other researchers to simulate CO_2 capture processes.

Fig. 5 illustrates the profile of the gas flow rate along the column. This result is not used for validation purposes because experimental data of gas flow rate inside the column were not reported in Tontiwachwuthikul et al. (1992).

Table 4 compares the results obtained from all proposed models in terms of outlet liquid temperature, rich solvent loading (CO_2 mol/MEA mol) and outlet CO_2 gas mole fraction.

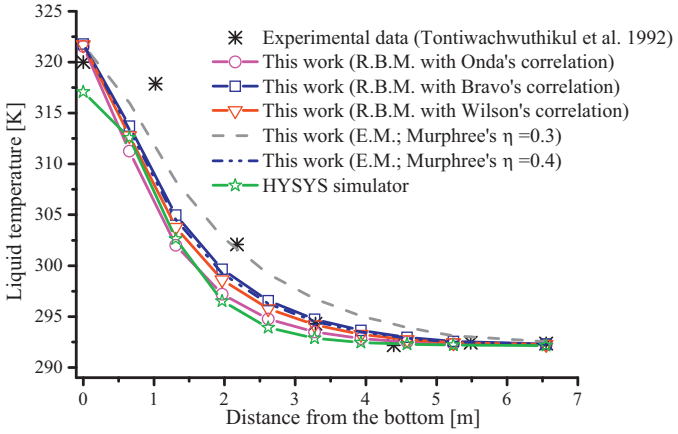

Fig. 2. Liquid temperature vs. distance from the bottom. Model validation for low flue-gas flow-rate.

Table 4
Simulated values obtained from all models.

Variables	Tontiwachwuthikul et al.	HYSYS®		This work									
				RBM						EM			
				Onda et al. (1968)		Bravo and Fair (1982)		Wilson (2004)		$\eta = 0.3$		$\eta = 0.4$	
		Valor	Error	Valor	Error	Valor	Error	Valor	Error	Valor	Error	Valor	Error
Outlet liquid temperature (K)	320.15	317.09	*0.96%*	321.559	*−0.44%*	321.781	*−0.51%*	321.715	*−0.49%*	321.691	*−0.48%*	321.761	*−0.50%*
Rich solvent loading (mol/mol)	0.443	0.419	*5.46%*	0.418	*5.91%*	0.416	*6.00%*	0.417	*5.78%*	0.409	*7.58%*	0.417	*5.91%*
CO_2 molar fraction (gas out)	0	6.30×10^{-5}	–	3.5×10^{-4}	–	1.4×10^{-3}	–	8.52×10^{-4}	–	5.5×10^{-3}	–	1.2×10^{-3}	–
CO_2 recovered (mol/s)	0.0268	2.67×10^{-2}	*0.16%*	0.0267	0.29%	0.0265	1.14%	0.0266	0.51%	0.0261	2.38%	0.0266	0.62%

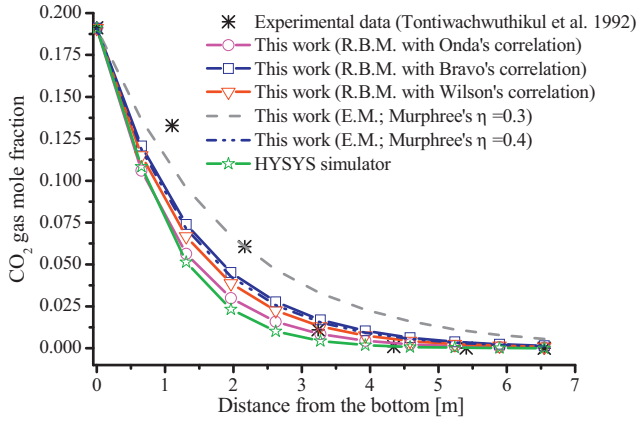

Fig. 3. CO_2 gas mole fraction vs. distance from the bottom. Model validation for low flue-gas flow-rate.

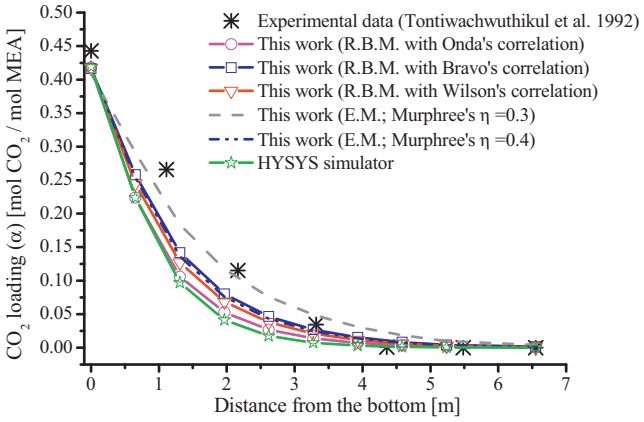

Fig. 4. CO_2 loading vs. distance from the bottom. Model validation for low flue-gas flow-rate.

4.1.2. *Model validation at medium flue-gas flow-rates*

As mentioned earlier, the model was also used to predict the performance of two medium scale absorption units operating in Kuwait. The design data of both units are taken from Alatiqi et al. (1994) who used the industrial data to successfully validate a rate based model assuming thermal non-equilibrium. Thus, validated solutions reported by Alatiqi et al. (1994) are used here to compare

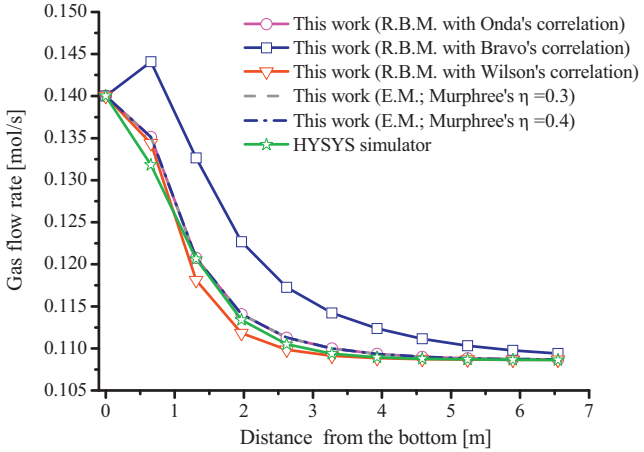

Fig. 5. Gas flow-rate vs. distance from the bottom. Model validation for low flue-gas flow-rate.

Table 5
Flue-gas specifications taken from Alatiqi et al. (1994).

	Flue-gas	Lean amine
Temperature (K)	322.05	310.95
Total flow-rate (kmol/h)	3338.85	18984.79
H_2O % (mole fraction)	0.73	92.61
CO_2% (mole fraction)	15.99	0.56
MEA % (mole fraction)	0.00	6.83
N_2% (mole fraction)	83.29	0.00
Pressure (kPa)	1482	1482

Absorber Unit of the Kuwait National Petroleum Company KNPC.

Table 6
Absorber specifications taken from Alatiqi et al. (1994).

Column type	Packed
Diameter (m)	2.74
Total packing height (m)	14.63
Stages number	10
Packing specifications	
Type of packed	Ceramic intalox saddles
Specific interfacial area (m^2/m^3)	625
Nominal packing size (m)	0.05
Void fraction	0.78

Absorption MEA units of the Kuwait National Petroleum Company KNPC).

the results obtained from our model, where thermal equilibrium is assumed.

The flue-gas conditions and absorber specifications corresponding to Kuwait National Petroleum Company Plant (KNPC) are summarized in Tables 5 and 6, respectively.

Figs. 6 and 7 compare the liquid temperature and CO_2 loading profiles along the absorber obtained by Alatiqi et al. (1994) with those predicted by our developed models.

Table 7 compares numerical values at the top and bottom of the absorber.

Finally, Table 8 compares the results for the other absorption unit corresponding to Petrochemical Industries Company (PIC) in Kuwait. Internal profiles of the process variables were not reported. Despite this, Figs. 8 and 9 are presented in order to give information on the gas phase. More specifically, the figures show the profiles of gas flow-rate and CO_2 gas mole fraction along the absorber.

The flue-gas specification and parameter values of the absorber are listed in Tables 9 and 10.

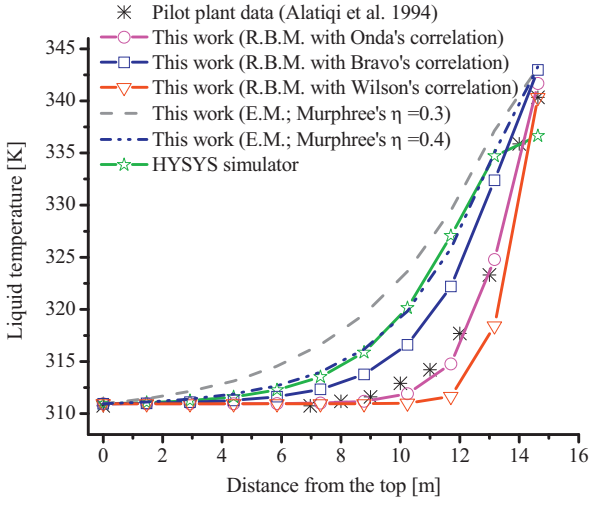

Fig. 6. Liquid temperature vs. distance from the bottom. Model validation for medium flue-gas flow-rate.

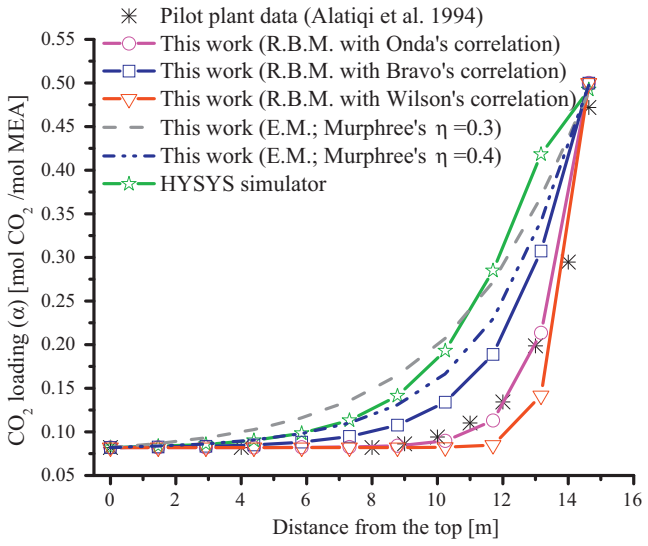

Fig. 7. CO_2 loading vs. distance from the bottom. Model validation for medium flue-gas flow-rate.

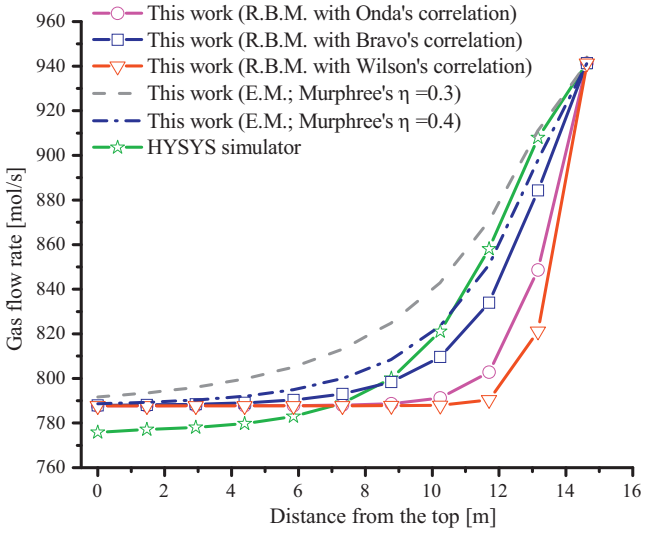

Fig. 8. Gas flow-rate vs. distance from the top of absorber. Model validation for medium flue-gas flow-rate.

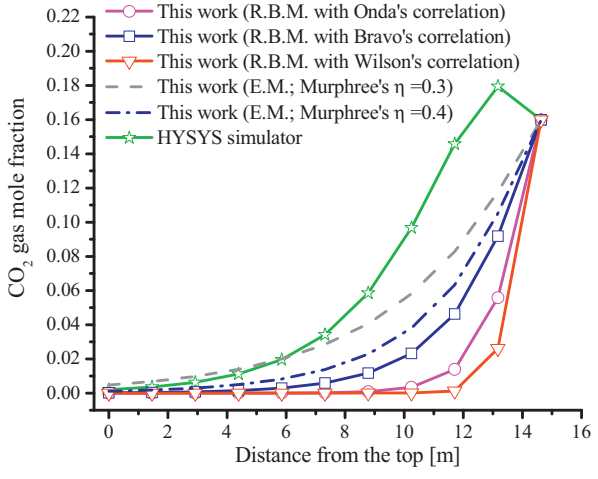

Fig. 9. CO_2 gas mole fraction vs. distance from the top of absorber. Model validation for medium flue-gas flow-rate.

Table 7
Comparison of results for KNPC unit.

	Design data (KNPC)	Rate-based model	This work					Hysys®
			RBM			EM		
	Alatiqi et al. (1994)		Onda et al. (1968)	Bravo and Fair (1982)	Wilson (2004)	$\eta = 0.3$	$\eta = 0.4$	
Outlet gas temperature (K)	322.050	323.050	310.950	310.995	310.950	311.438	311.120	311.029
Outlet liquid temperature (K)	–	340.350	336.980	342.973	340.323	343.176	343.285	336.670
Rich solvent loading (mol/mol)	–	0.4720	0.5000	0.4996	0.5000	0.4895	0.4977	0.4928
CO_2 mole fraction (gas out)	<0.0001	8.90×10^{-7}	7.48×10^{-7}	1.87×10^{-4}	5.51×10^{-7}	4.78×10^{-3}	1.06×10^{-3}	5.07×10^{-4}
H_2O mole fraction (gas out)	<0.00045	4.34×10^{-3}	4.72×10^{-3}	4.73×10^{-3}	4.72×10^{-3}	4.85×10^{-3}	4.76×10^{-3}	4.43×10^{-3}
CO_2 recovered (mol/s)	–	148.2041	150.5061	150.3595	150.63	146.7249	149.6669	148.5964

Table 8
Comparison of results for PIC unit.

	Design data (PIC)	Rate-based model	This work					Hysys®
			RBM			EM		
	Alatiqi et al. (1994)		Onda et al. (1968)	Bravo and Fair (1982)	Wilson (2004)	$\eta = 0.3$	$\eta = 0.4$	
Outlet gas temperature (K)	316.150	317.850	314.194	314.295	314.223	314.505	314.270	314.322
Outlet liquid temperature (K)	–	334.150	339.989	340.210	340.098	340.128	340.186	333.639
Rich solvent loading (mol/mol)	–	0.4810	0.4995	0.4975	0.4990	0.4911	0.4981	0.5435
CO_2 mole fraction (gas out)	–	7.80×10^{-7}	3.41×10^{-4}	1.63×10^{-3}	6.52×10^{-4}	5.77×10^{-3}	1.26×10^{-3}	1.99×10^{-3}
H_2O mole fraction (gas out)	4.80×10^{-3}	3.36×10^{-3}	4.73×10^{-3}	4.75×10^{-3}	4.74×10^{-3}	4.81×10^{-3}	4.75×10^{-3}	4.39×10^{-3}
CO_2 recovered (mol/s)	–	146.3097	146.3895	145.4281	146.0060	142.9615	145.6450	145.2129

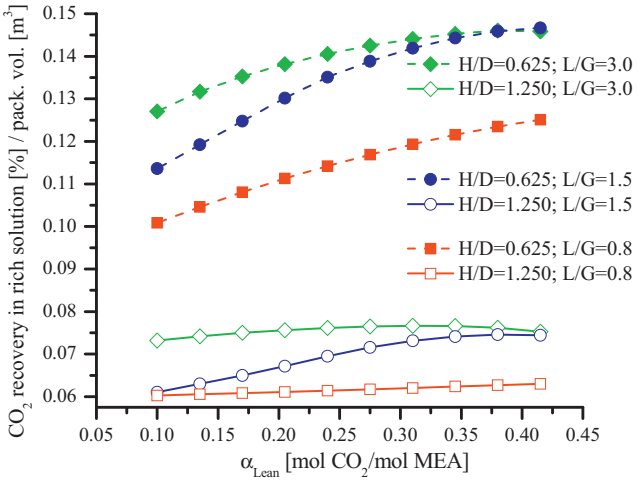

Fig. 10. Variation of the ratio between the CO_2 recovery in rich solution and packing volume with the model parameters (optimized cases).

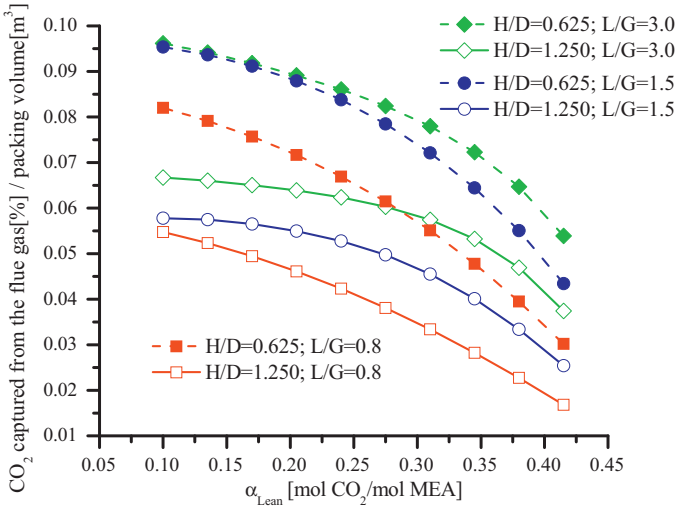

Fig. 11. Variation of the ratio between the CO_2 removed from the flue-gas and packing volume with the model parameters (optimized cases).

4.2. Example 2: optimization problem

The proposed RBM model (Eqs. (1)–(30)) involving the Onda's correlation is used to determine the optimal design that maximizes the ratio between the CO_2 recovery in rich solution and the packing volume, as it was formulated in Section 3. Thus, the model is solved by varying several parameters (α_{lean}, H/D, L/G, T_{lean}). Then, the optimal values of the main process variables (CO_2 recovery in rich solution, CO_2 removed from the gas phase, liquid temperature, packing volume, pressure drop along the absorber, among others) are shown in terms of the assumed parameters in separate figures, more specifically from Figs. 10–27.

The gas specification used for optimizations is listed in Table 11.

Table 9
Flue-gas specifications for the absorber unit of the PIC.

	Flue gas	Lean amine
Temperature (K)	316.15	314.15
Total flow-rate (kmol/h)	2656.21	22478.1
H_2O % (mole fraction)	0.48	93.11
CO_2 % (mole fraction)	19.84	0.74
MEA % (mole fraction)	0.00	6.15
N_2 % (mole fraction)	79.67	0.00
Pressure (kPa)	1819	1819

Taken from Alatiqi et al. (1994).

Table 10
Absorber parameter values.

Column type	Packed
Diameter (m)	2.44
Total packing height (m)	24.15
Stages number	10
Packing specifications	
Type of packed	Ceramic intalox saddles
Specific area (m^2/m^3)	625
Nominal packing size (m)	0.05
Surface tension (N/m)	0.061

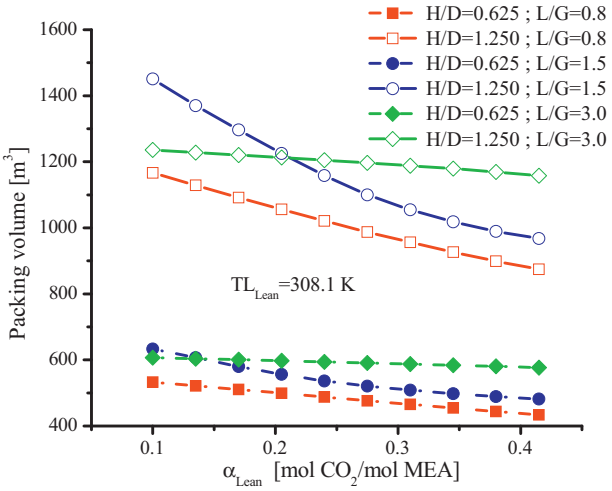

Fig. 12. Optimal packing volumes vs. α_{lean} for different H/D and L/G ratios (T_{lean} = 308.1 K).

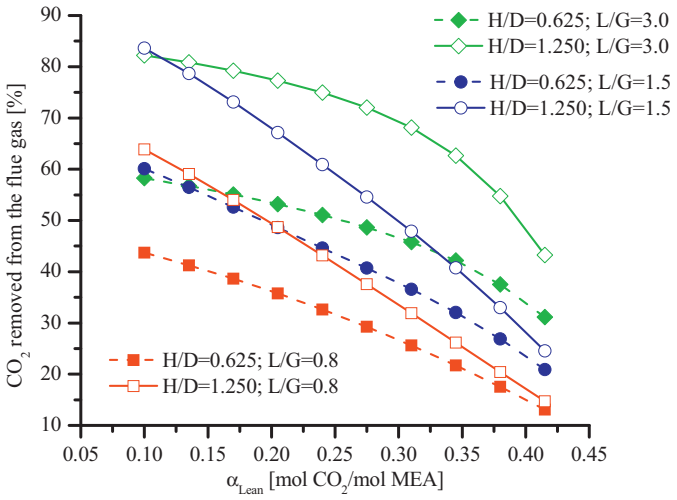

Fig. 14. Optimal CO_2 removed from flue-gas stream vs. α_{lean} for different H/D and L/G ratios (T_{lean} = 308.1 K).

Table 11
Flue-gas specifications.

Gas flow-rate (mol/s)	8000
Inlet temperature (K)	303.15
CO_2 (mole fraction)	0.04
H_2O (mole fraction)	0.0845

Despite that, the results obtained for two values of H/D (height/diameter) are here presented, it should be clear that H/D was considered as an optimization variable in the proposed model. As expected, in all cases H/D reached its lower bound because the packing volume is explicitly considered in the objective function (minimization). Thus, the developed model was solved for two lower bounds (0.625 and 1.250).

The effect of the main process parameters on the absorption performance is discussed as follows.

4.2.1. Effect of H/D and L/G ratios and CO_2 loading (α_{lean}) on the objective function, CO_2 recovery, packing volume and total pressure drop

Figs. 10–14 show the influence of α_{lean}, H/D and L/G ratios on the total packing volume and absorption efficiency. The corresponding optimal values of the rich amine temperature, the outlet CO_2

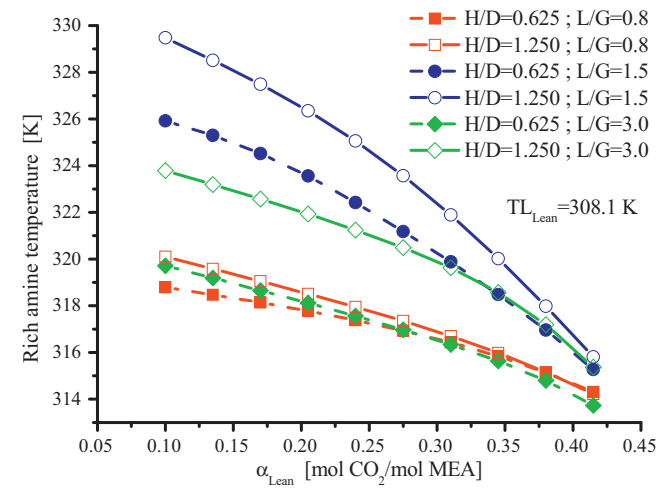

Fig. 15. Optimal rich amine temperature vs. α_{lean} for different H/D and L/G ratios (T_{lean} = 308.1 K).

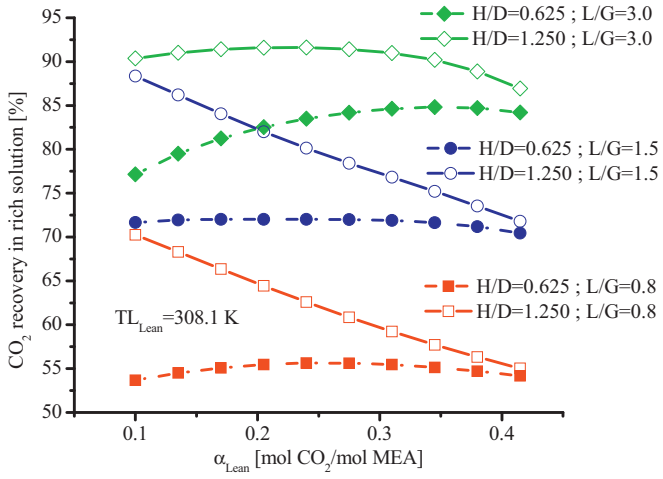

Fig. 13. Optimal CO_2 recoveries in rich solution vs. α_{lean} for different H/D and L/G ratios (T_{lean} = 308.1 K).

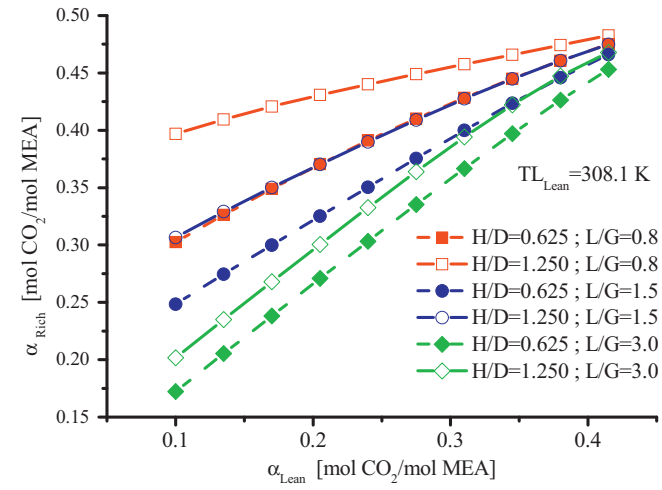

Fig. 16. Optimal α_{rich} values vs. α_{lean} for different H/D and L/G ratios (T_{lean} = 308.1 K).

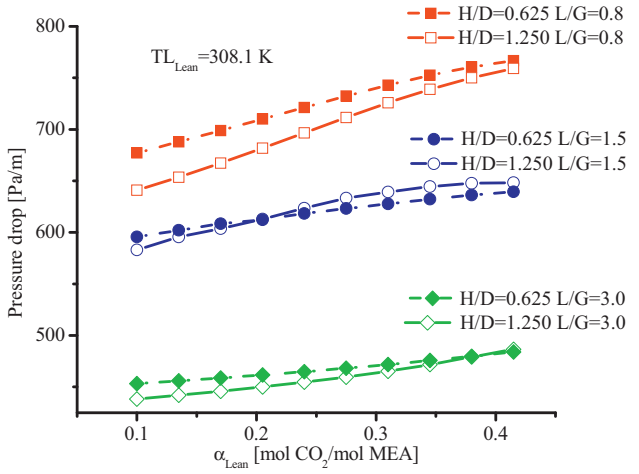

Fig. 17. Optimal total pressure drop vs. α_{lean} for different H/D and L/G ratios (T_{lean} = 308.1 K).

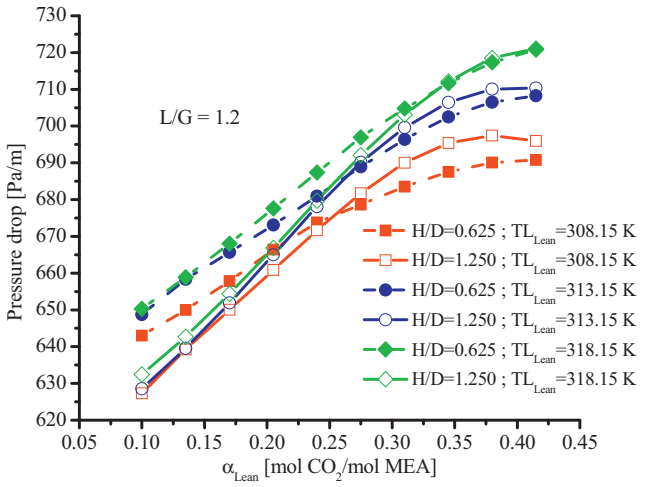

Fig. 20. Optimal total pressure drop vs. α_{lean} for different H/D ratio and T_{lean} (L/G = 1.20).

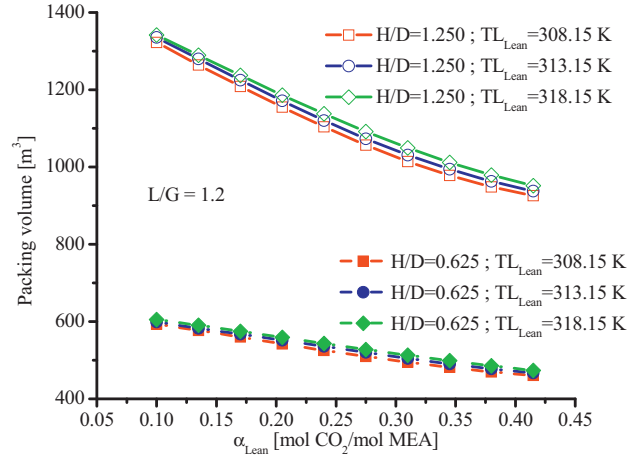

Fig. 18. Optimal packing volumes vs. α_{lean} for different H/D ratio and T_{lean} (L/G = 1.20).

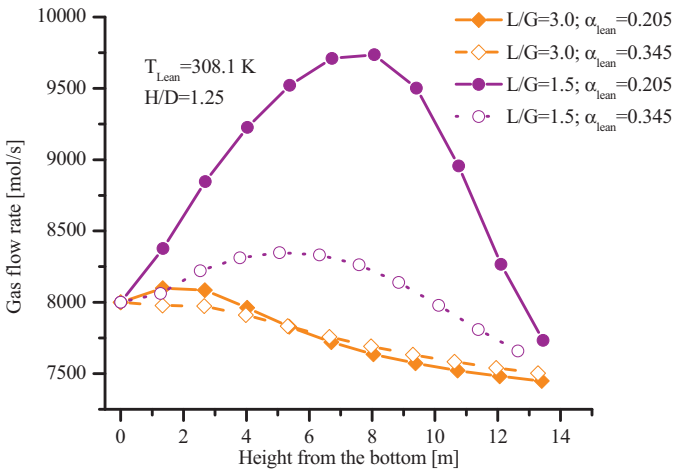

Fig. 21. Profile of the gas flow-rate along the column for different values of L/G and α_{lean}.

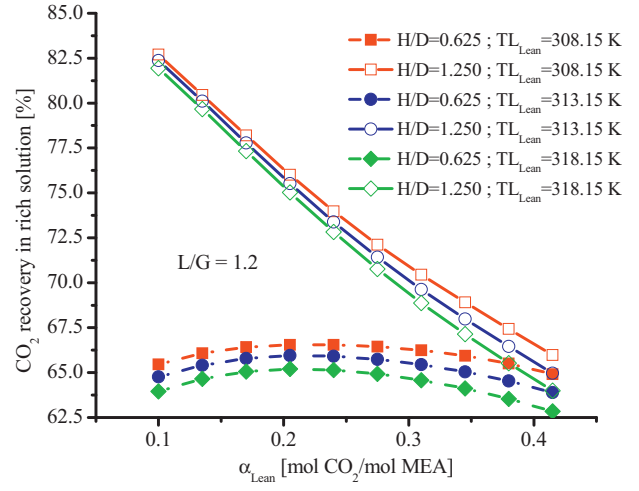

Fig. 19. Optimal CO_2 recoveries vs. α_{lean} for different H/D ratio and T_{lean} (L/G = 1.20).

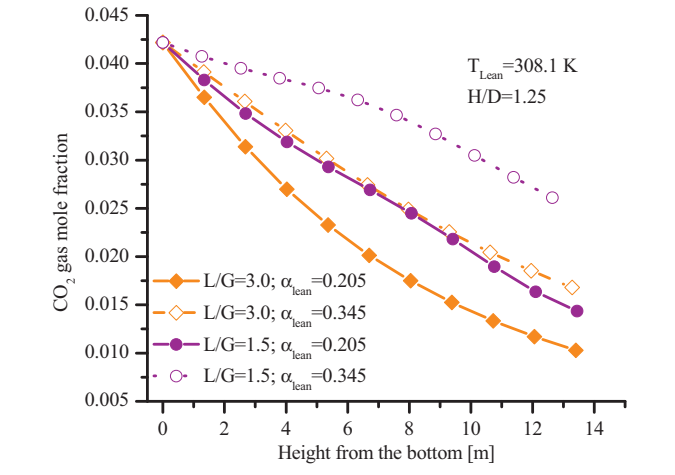

Fig. 22. Profile of the CO_2 gas mole fraction along the column for different values of L/G and α_{lean}.

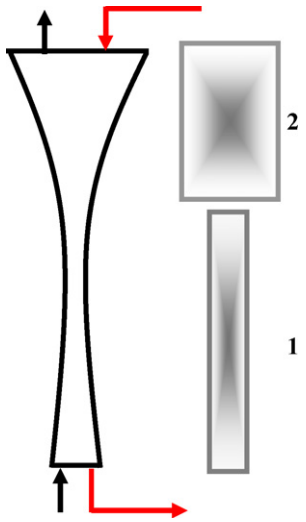

Fig. 23. Schematic representation of the variation of diameter along the absorber.

loading (α_{rich}) and total pressure drop are illustrated from Figs. 15–17.

4.2.2. Effect of dimension ratio (H/D), lean solution temperature (T_{lean}) and inlet CO_2 loading (α_{lean}) on the CO_2 recovery, packing volume and total pressure drop

Optimal results obtained for three amine solution temperatures (308.15, 313.15 and 318.15 K) and two H/D ratios (0.625 and 1.250) are presented in Figs. 18–20.

Figs. 21 and 22 show the profiles of gas flow-rate and CO_2 gas mole fraction along the absorber in terms of L/G and α_{lean}.

4.2.3. Optimal design considering a diameter distribution along the height of the absorber

In the optimized results presented in the previous section the diameter of column was considered as an optimization variable and its optimal value was obtained as result. It was also assumed a same diameter along the absorber height (Eq. (26)).

In order to investigate the effect of the diameter variation on the absorption efficiency, the proposed model was also solved to minimize the packing volume but now with the possibility of obtaining a diameter distribution along the height of the absorber. In other words, the diameter may change at different points along the column. For this purpose, Eq. (26) was removed from the model. As will be analyzed in Section 5.2.3, two optimization problems are proposed. If the optimal solution indicates that the variation of the diameter along the absorber improves the process efficiency

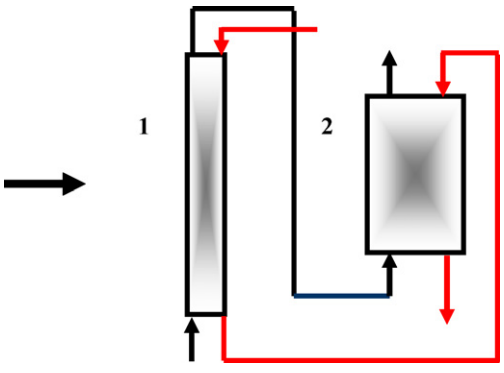

Fig. 24. Alternative arrangement for the absorption process.

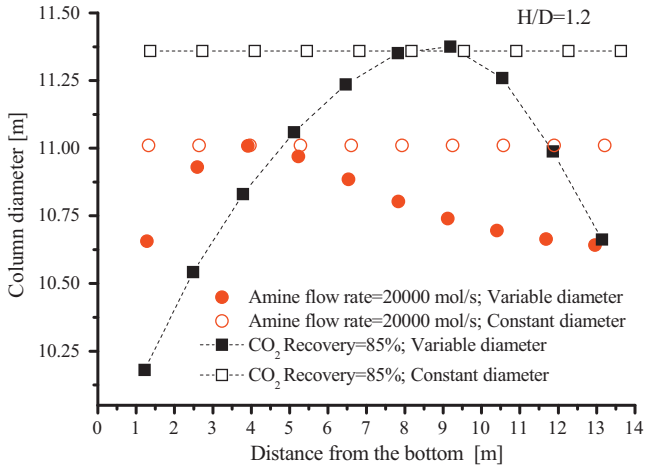

Fig. 25. Optimal diameter distributions along the absorber for $H/D = 1.20$.

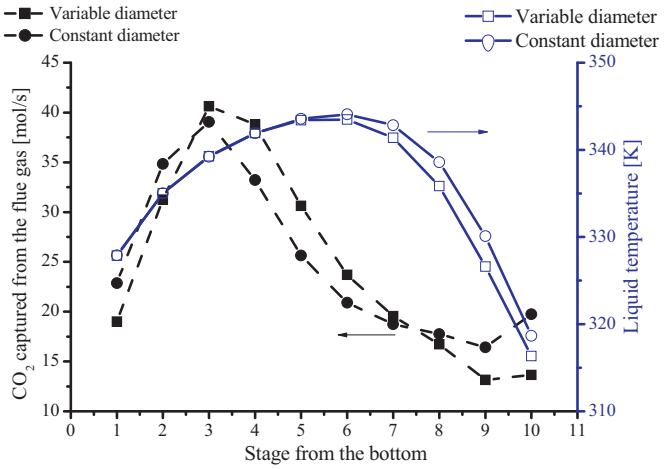

Fig. 26. Optimal profiles of the amount of CO_2 recovered and liquid temperature along the absorber ($H/D = 1.20$).

(Fig. 23), it is interesting to study how the solution could be implemented for a real design (Fig. 24).

Optimizations have been performed varying the H/D ratio, the CO_2 recovery in rich solution and the amine flow-rate. Precisely, for the case where the amine flow rate was fixed (20,000 mol/s),

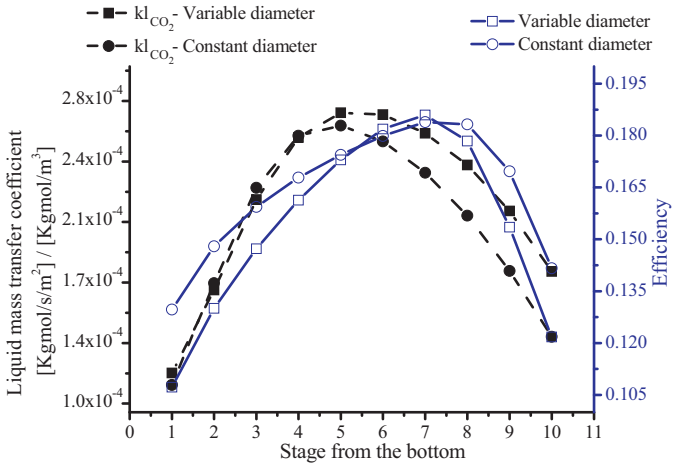

Fig. 27. Optimal values of transfer mass coefficient and efficiency along the absorber ($H/D = 1.20$).

Table 12
Heigths of stages (m).

Stage	CO_2 recovery = 85%				Amine flow rate = 20,000 mol/s			
	H/D = 0.8		H/D = 1.2		H/D = 0.8		H/D = 1.2	
	Constant diameter	Variable diameter	Constant diameter	Variable diameter	Constant diameter	Variable diameter	Constant diameter	Variable diameter
1	0.881	0.866	1.363	1.222	0.876	0.855	1.321	1.279
2	1.762	1.746	2.726	2.487	1.752	1.726	2.643	2.590
3	2.642	2.629	4.089	3.786	2.628	2.602	3.964	3.912
4	3.523	3.509	5.452	5.113	3.503	3.476	5.285	5.228
5	4.404	4.385	6.816	6.462	4.379	4.345	6.606	6.534
6	5.285	5.258	8.179	7.824	5.255	5.210	7.928	7.831
7	6.165	6.127	9.542	9.189	6.131	6.072	9.249	9.119
8	7.046	6.994	10.905	10.540	7.007	6.930	10.570	10.403
9	7.927	7.859	12.268	11.859	7.883	7.786	11.892	11.682
10	8.808	8.723	13.631	13.138	8.759	8.641	13.213	12.959

the CO_2 recovery in rich solution was considered as optimization variable in order to avoid infeasible solutions and vice versa, the amine flow rate was considered as an optimization variable when the CO_2 recovery in rich solution was fixed (85%). The same gas specification considered previously was also used for optimizations (Table 11).

Fig. 25 shows the optimal diameter distributions along the absorber obtained for all cases. For clarity, the figures show the profiles through the stages (x-axis) instead of height. The corresponding height of each stage is listed in Table 12.

For the case study with H/D = 1.2 and 85% of CO_2 recovery in rich solution, Tables 12 and 13 compare the optimal values of the most important process variables obtained considering both diameter distribution along the absorber and constant diameter.

The following figures compare the optimal profiles of the amount of CO_2 recovered in rich solution, liquid temperature, transfer mass coefficient and efficiency along the absorber obtained for both constant and variable diameters and H/D = 1.2.

Finally, Table 14 reports the optimal values obtained by fixing the amine flow rate at 20,000 mol/s (CO_2 recovery in rich solution considered as free).

5. Discussion

5.1. Discussion of model validation

5.1.1. Model validation at low flue-gas flow-rate

Seven experimental values of temperature and CO_2 gas mole fraction along the column were used for validation purpose. For a better comparison, the output results obtained by EM and RBM models and experimental data were compared for two sections of the column: at the bottom and at the middle-top of column.

Figs. 2 and 3 clearly show that the equilibrium model (EM) with Murphree's efficiency (η) fixed at 30% predicts better results than the other models at the bottom of column (from 0 to 2.10 m) for the liquid temperature and CO_2 mole fraction profiles. It should be mentioned, however, that the RBM accurately predicted these values and the difference in the numerical values predicted by both models is small. The experimental data at the middle of the absorber (from 2.10 to 4.5 m) are well predicted by the rate based models and the equilibrium models.

On the other hand, a correct prediction of the CO_2 mole fraction profile along the column is obtained by using EM with η fixed at 30% (Fig. 3). From this figure can also be shown that the rate based models and EM with η fixed at 40% predict correct results from 3.2 to 6.55 m (from the bottom of the column).

Fig. 4 shows same trends of predicted values for the rich solvent loading (α) profile along the absorber.

From Table 4, where simulated values of temperature and compositions of the leaving streams are listed, it can be concluded that the numerical values predicted by all models (EM and RBM) are essentially the same and are very close to the experimental values. In addition, Table 4 shows that the obtained values for the streams leaving the absorber are not dependent on the correlation used to compute the effective interfacial area for mass transfer.

As mentioned earlier, Fig. 5 is presented in order to illustrate the profile of the gas flow rate along the column but not for validation purpose because experimental data of gas flow rate inside the column were not reported in Tontiwachwuthikul et al. (1992).

Briefly, the following conclusions can be drawn from the obtained results for low flue-gas flow-rate analyzed in this example.

From the profiles illustrated in Figs. 2–4 it can be concluded that both EM and RBM models accurately predict the experimental data for low gas flow-rate.

Contrary to the expected, the validation results clearly show that the experimental values are satisfactorily predicted by simple mathematical models, in this case equilibrium models (EM). Certainly, the results obtained by EM are in accordance with those obtained by RBM and experimental data. This fact is important from a mathematical modeling point of view and complexity involved in attempting to solve both models; EM is preferred over RBM because it requires fewer equations and variables and consequently the computational effort required to solve EM is less than RBM. But, it should be stressed, however, that if data required and reliable methods are available, RBM models are more appropriate to gain more understanding and insights on the mechanisms for mass, energy and momentum transfers. Thus, for low flow-rate,

Table 13
Optimal values obtained with diameter distribution and constant diameter (CO_2 recovery = 85%).

H/D	Recovery (%)	Amine flow rate (mol/s)		Volume (m^3)		Height (m)	
		Variable diameter	Constant diameter	Variable diameter	Constant diameter	Variable diameter	Constant diameter
0.8[a]	85.00[b]	22377.97	21723.72 *(−2.92%)*	814.60	838.47 *(2.8%)*	8.72	8.81
1.2[a]		13143.68	12438.48 *(−5.36%)*	1241.17	1381.39 *(10.15%)*	13.14	13.63

[a] Lower bound.
[b] Fixed value.

Table 14
Optimal values obtained with diameter distribution and constant diameter (solvent flow-rate = 20,000 mol/s).

H/D	Amine flow rate (mol/s)	Recovery (%)		Volume (m^3)		Height (m)	
		Variable diameter	Constant diameter	Variable diameter	Constant diameter	Variable diameter	Constant diameter
0.8[a]	20000.00[b]	83.52	83.97	791.93 *(−3.9%)*	824.54	8.64	8.76
1.2[a]		89.83	90.39	1187.65 *(−5.60%)*	1258.13	12.96	13.21

[a] Lower bound.
[b] Fixed.

the use of EM or RBM depends on the goals and purposes of the user.

Finally, it is mentioned that all developed models are flexible enough, allowing to perform all simulations without computational problems.

5.1.2. Model validation at medium flue-gas flow-rates

As is clearly shown in Figs. 6 and 7, the profiles of temperature and CO_2 loading predicted by the RBM considering Onda's correlations are similar to those reported by Alatiqi et al. (1994). The comparisons also show that predicted results are strongly influenced by the correlation used to compute the effective interfacial area. For instance, the use of the Wilson's correlation in the RBM model predicted accurately the liquid temperature and CO_2 loading values from the top of absorber to 10.00 m. But it under predicted the profiles from 10 to 14.6 m. In contrast to this, RBM with Bravo's correlation, EM models (η = 30 and 40%) and HYSYS simulator over predicted the values reported by Alatiqi et al. (1994) significantly.

According to the simulated results listed in Table 7, a similar value reported by Alatiqi et al. (1994) for the outlet liquid temperature is predicted using Wilson's correlation. Onda's correlation, which accurately predicts the temperature profile along the column, under predicts the outlet liquid temperature by 3.4 °C. Equilibrium models over predicts the temperature value by 3 °C.

The outlet CO_2 mole fraction is well predicted by both Onda and Wilson's correlations.

The profiles of gas flow-rate and CO_2 gas mole fraction along the absorber corresponding to Figs. 6 and 7 are illustrated in Figs. 8 and 9, respectively. Experimental data of these process variables are not included in the figures because they were not reported by Alatiqi et al. (1994). As shown, both profiles increase as the height from the top increase, following the same trends observed for the liquid temperature and CO_2 loading (Figs. 6 and 7).In summary, the findings from this validation study indicate that in order to study the behavior of the CO_2 absorption inside the absorber, the rate based model involving Onda's correlation is more suitable than Bravo and Wilson's correlations. Thus, it can be used for control design and to study the dynamic behavior of the absorption process. It should be mentioned, however, that the proposed RBM model involving Wilson's correlation can be correctly used to predict specification's values of liquid and vapor streams that leave the absorber.

For the medium flue-gas flow-rate analyzed in this section, the obtained results clearly show that RBM models are preferred than EM models to study the absorption process, in contrast to what happens at low flue-gas flow-rate.

5.2. Discussion of optimizations

5.2.1. Influence of H/D and L/G ratios on the optimal values of the objective function, CO_2 loading, packing volume and total pressure drop

Fig. 10 clearly shows that for $H/D = 0.625$ and for all L/G ratios the objective function (CO_2 recovery in rich solution/packing volume) increases as α_{lean} increases. For $H/D = 1.250$ and $L/G = 0.800$ and 3.000, the objective function keeps almost constant with the increasing of α_{lean} and a slight increase is observed for $H/D = 1.250$ and $L/G = 1.5$. On the other hand, Fig. 11 shows the variation of the ratio of the CO_2 removed from the flue-gas and packing volume vs. α_{lean}. As expected, this ratio decreases as α_{lean} increases in all cases.

Figs. 12–14 show how the packing volume, the CO_2 recovery in rich solution and CO_2 removed from the flue-gas stream vary for each one of the parameter values. As can be seen, different trends are observed for CO_2 recovery in rich solution (Fig. 13) and CO_2 removed from the flue-gas stream (Fig. 14). In all cases, the amount of CO_2 removed from the flue-gas stream decrease with the increasing α_{lean} (Fig. 14); but in some cases the CO_2 recovery in rich solution increases or remains constant as α_{lean} increases (Fig. 13).

From optimal results shown in Figs. 12 and 13, it can be observed that in the range of $\alpha_{lean} = 0.1$ to $\alpha_{lean} = 0.2$, high CO_2 recoveries in rich solution do not require high packing volumes. Certainly, for $H/D = 1.25$, the minimum packing volume to maximize the CO_2 recovery in rich solution is 1250 m^3 instead of 1400–1250 m^3 but this requires to operate the absorber with $L/G = 3$ instead of $L/G = 1.5$.

Also, for $H/D = 1.25$ and $L/G = 3$, Fig. 13 show that the CO_2 recovery in rich solution and packing volume are not significantly affected by α_{lean}. In contrast to this, for $H/D = 1.25$ and $L/G = 1.5$; $H/D = 0.625$ and $L/G = 3$; $H/D = 1.25$ and $L/G = 0.8$; these parameters are significantly influenced by α_{lean} in different ways. For instance, for the following two cases: (a) $H/D = 1.25$ and $L/G = 1.5$, (b) $H/D = 1.25$ and $L/G = 0.8$, the CO_2 recovery in rich solution and packing volume decrease as the α_{lean} increases. However, for $H/D = 0.625$ and $L/G = 3$, the CO_2 recovery in rich solution increase as the increasing of α_{lean} while the packing volume is not significantly influenced. Opposite effects are observed for $H/D = 0.625$ and $L/G = 1.5$, where the packing volume decrease as the increasing of α_{lean} while the CO_2 recovery in rich solution is not affected.

Finally, it is interesting to observe the effect of H/D ratios and α_{lean} on the CO_2 recovery in rich solution and packing volume for given L/G ratios. For a same L/G ratio, the maximum difference on the CO_2 recovery in rich solution is observed at $\alpha_{lean} = 0.1$ and from this value the difference decreases with the increasing of α_{lean}. In all cases, the minimum difference is observed at $\alpha_{lean} = 0.4$ and the obtained results indicate that, for same values of L/G ratios, similar CO_2 recovery in rich solution can be achieved requiring almost half of packing volumes (Fig. 12). Thus, for α_{lean} values greater than 0.24 and fixed L/G ratio, the H/D ratio plays an important role, preferring lower H/D ratios to minimize the packing volume and maximize the CO_2 recovery in rich solution (Figs. 12 and 13).

5.2.2. Influence of the H/D ratio, the lean solution temperature and the inlet CO_2 loading on the optimal values of CO_2 loading, packing volume and total pressure drop

According to the results shown in Figs. 18–20, it can be concluded that T_{lean} has not significant effect on the CO_2 recovery in rich solution and packing volume as well. Certainly, slight differences on the CO_2 recoveries in rich solution and pressure drops are observed from $\alpha_{lean} = 0.25$.

Figs. 21 and 22 show how the total gas flow-rate and CO_2 gas mole fraction vary along the column for two values of L/G and α_{lean}. As shown, the total gas flow-rate reaches a maximum value which depends on the values of L/G ratios and α_{lean}.

5.2.3. Optimal diameter distribution through the height of the absorber

The intention of this analysis is to identify alternative designs for the absorption process. For this, the proposed optimization model is solved by removing Eq. (26) in order to study how the diameter variation along the column affects the absorption efficiency. If the diameter varies significantly along the absorber (Fig. 23) and the absorption efficiency is improved, it may be possible to mountain two columns with different diameters and heights but with constant diameter in each one of the absorbers, as is shown in Fig. 24. This configuration may be beneficial because, keeping the process efficiency, it reduces the risk of the channeling of vapor and liquid streams which causes operating problems in tall packed absorbers.

In addition the study of the influence of the variation of the diameter along the column on the absorption is also valuable from a solution strategy point of view. The optimal values obtained when the diameter along the absorber varies are lower and upper bounds for practical optimizations, for example a constant diameter along the column. Therefore, these solutions can be efficiently used not only to initialize the model variables but also to reduce the size of the optimization search space for practical optimizations.

The following optimization problems were investigated:

- Minimization of packing volume, for $H/D = 0.8$ and 1.2; CO_2 recovery in rich solution = 85%.
- Minimization of packing volume, for $H/D = 0.8$ and 1.2; amine solution flow-rate = 20,000 mol/s.

Both optimization problems were solved for constant and variable diameters along the absorber.

As shown in Fig. 25, different optimal profiles are obtained which strongly depend on the fixed parameter values. For example, for $H/D = 1.2$ and 85% of CO_2 recovery in rich solution, the maximum value of diameter (11.4 m) occurs at 9.10 m from the bottom of the absorber. For this case, the difference of diameter inside the column is about 10–11%. For the remaining study case, despite the existence of optimal diameter profile, the variation on the distributions is not quite significant.

According to Table 12, for both H/D ratios, the absorber design considering an optimal diameter distribution is preferred because it involves the lowest packing volume. Certainly, for $H/D = 0.8$ and $H/D = 1.2$ the packing volumes decrease by 3% and 10% respectively. It should be mentioned, however, the amine flow rates increase by 3% and 5.4%, which may have significant impact on the operating cost of the amine regeneration (reboiler heat duty). In addition, it is interesting to investigate for this specific optimization problem, if using two absorbers with smaller dimensions (with constant diameters in both absorbers but different) in comparison to that needed by one column, the efficiency is still kept. Also, it should be mentioned that for a techno-economical design it is necessary to optimize the whole CO_2 capture process considering an economic aspect in the objective function (investment and operating costs). The feasibility and effectiveness of this scheme taking into account the criteria mentioned above will be further investigated in detail.

Finally, from Table 14 which reports the optimal values obtained by fixing the amine flow rate at 20,000 mol/s (CO_2 recovery in rich solution considered as free), it is also observed that a diameter distribution inside the column leads to decrease the packing volume, for a similar CO_2 removal.

6. Conclusions – future works

A deterministic NLP mathematical model for the reactive CO_2 absorption into aqueous MEA solutions was presented. Temperature, composition and flow-rate of liquid and gas streams through the length of the absorber as well as dimensions and total pressure drop were considered as optimization variables. The proposed rate based model is a valuable tool not only to optimize the process but also to simulate the absorption process if the degree of freedom of the equation system is zero.

The output results were validated for low and medium flue-gas flow-rates by comparing predicted values with experimental data. The effect of different model hypothesis on the CO_2 absorption efficiency has been investigated.

From the validation results obtained for low flue-gas flow-rate (0.14 mol/s) it was shown both models (EM and RBM) predict accurately the behavior of the absorption process. The EM may be preferred over RBM if the model size is considered; the number of equations and variables involved by EM are smaller than RBM. However, for medium-high flow rate the RBM is always preferred over EM because the experimental data are more accurately predicted. More specifically, RBM involving Onda's correlation is more suitable than Bravo and Wilson's in order to study the behavior of the CO_2 absorption inside the absorber. However, RBM involving Wilson's correlation can be used to predict specification's values of liquid and vapor streams that leave the absorber. Thus, the selection of the appropriate correlation depends on the purpose of the user.

After validation, the robustness and flexibility of the model as well as the used NLP solver (CONOPT) has been examined by solving an optimization problem. It consisted in determining operating conditions and dimensions in order to maximize the ratio between the CO_2 recovery in rich solution and the packing volume column for given flue-gas conditions (flow-rate, temperature and compositions). The effect of the main process parameters on the optimal solutions was investigated.

Obtained results showed that an optimal diameter distribution along the absorber improves the CO_2 absorption efficiency. Certainly, for same CO_2 recoveries in rich solution, optimal diameter distributions reduced the packing volumes. Depending on the case studies where different specifications were considered, the packing volumes decrease from 3 to 10% in comparison with a constant diameter along the absorber. Then, it is interesting to study in detail the feasibility and how this solution may be implemented for real designs. For big columns (tall and/or high diameter columns) it is clear that two or more absorption trains (and one or more sections for each column) may be necessary. Also, this fact can be mentioned for the CO_2 compression stage. In addition, from a process availability point of view it could be important to design more than one absorption and compression train. An optimization problem considering all these variables (number of absorption/desorption and compression trains) is very complex involving many discrete decisions leading to a high combinatorial problem. Here, the effect of a continuous variation of the column diameter can be used as an indicator of the benefit of introducing (or not) further considerations about column sections in more elaborated optimization problems.

Despite the good agreement between the model output results to those obtained by experimental works, the proposed model will be extended to improve the mass and energy transfer between phases. In addition, the model will be properly extended to study the effect of other reaction mechanisms in the absorption efficiency. The use of blending amines as solvent and the coupling of the post-combustion process into power plants are other interesting points to consider in future works.

Acknowledgements

Financial supports obtained from the Consejo Nacional de Investigaciones Científicas y Técnicas (CONICET), the Agencia Nacional

para la Promoción de la Ciencia y la Tecnología (ANPCyT), the Universidad Tecnológica Nacional Facultad Regional Rosario (UTN-FRRo) Argentina are greatly acknowledged.

References

Aboudheir, A., Tontiwachwuthikul, P., Chakma, A., Idem, R., 2003. Kinetic of reactive absorption of carbon dioxide in high CO_2-loaded, concentrated aqueous monoethenolamine solutions. Chemical Engineering Science 58, 5195–5210.

Alatiqi, I., Sabri, M.Fk., Bouhamra, W., Alper, E., 1994. Steady-state rate-based modelling for CO_2/amine absorption–desorption systems. Gas Separation & Purification 8, 3–11.

Asprion, N., 2006. Nonequilibrium rate-based simulation of reactive systems: simulation model, heat transfer, and influence of film discretization. Industrial & Engineering Chemistry Research 45, 2054–2069.

Austgen, D.M., 1989. A model of vapor–liquid equilibria for acid gas–alkanolamine–H_2O systems. Ph.D. dissertation, http://www.che.utexas.edu/rochelle_group/Pubs/Austgen%20Diss.pdf.

Bedell, S., 2011. Amine autoxidation in flue gas CO_2 capture – mechanistic lessons learned from other gas treating processes. International Journal of Greenhouse Gas Control 5 (1), 1–6.

Bravo, J.L., Fair, J.R., 1982. Generalized correlation for mass transfer in packed distillation columns. Industrial & Engineering Chemistry Process Design and Development 21, 162–170.

Brooke, A., Kendrick, D., Meeraus, A., 1996. GAMS – A User's guide (Release 2.25). The Scientific Press, San Francisco, CA.

Chakravarty, T., Phukan, U.K., Weiland, R.H., 1985. Reaction of acid gases with mixtures of amines. Chemical Engineering Progress 81, 32–36.

deMontigny, D., Aboudheir, A., Tontiwachwuthikul, P., Chakma, A., 2006. Modelling the performance of a CO_2 absorber containing structured packing. Industrial & Engineering Chemistry Research 45, 2594–2600.

Dugas, R., 2006. Pilot plant study of carbon dioxide capture by aqueous monoethanolamine. M.S.E. Thesis, http://www.che.utexas.edu/rochelle_group/Pubs/Dugas_DOE_2006.pdf.

Drud, A.S., 1992. CONOPT, A GRG Code for Large scale Nonlinear Optimization Reference Manual. ARKI Consulting and Development A/S, Bagsvaerd, Denmark.

Edali, M., Aboudheir, A., Idem, R., 2009. Kinetics of carbon dioxide absorption into mixed aqueous solutions of MDEA and MEA using a laminar jet apparatus and a numerically solved 2D absorption rate/kinetics model. International Journal of Greenhouse Gas Control 3, 550–560.

Faramarzi, L., Kontogeorgis, G.M., Michelsen, M.L., Thomsen, K., Stenby, E.H., 2010. Absorber model for CO_2 capture by monoethanolamine. Industrial & Engineering Chemistry Research 49, 3751–3759.

Freguia, S., 2002. Modeling of CO_2 removal from flue gases using MEA. M.S. thesis, University of Texas at Austin, http://www.che.utexas.edu/rochelle_group/Pubs/FreguiaPubThesis.pdf.

Greer, T., 2008. Modeling and Simulation of Post Combustion CO_2 Capturing. Ph.D. thesis, Telemark University College, Faculty of Technology, Porsgrunn, Norway.

Hilliard, M.D., 2008. A predictive thermodynamic model for an aqueous blend of potassium carbonate, piperazine and monoethanolamine for carbon dioxide capture from flue gas. Ph.D. dissertation, University of Texas of Austin.

Kister, H.Z., 1992. Destillation Design. McGraw Hill, USA.

Kucka, L., Kenig, E.Y., Górak, A., 2002. Kinetics of the gas–liquid reaction between carbon dioxide and hydroxide ions. Industrial & Engineering Chemistry Research 41, 5952–5957.

Kucka, L., Müller, I., Kenig, E.Y., Górak, A., 2003. On the modeling and simulation of sour gas absorption by aqueous amine solutions. Chemical Engineering Science 58, 3571–3578.

Lawal, A., Wang, M., Stephenson, P., Yeung, H., 2009. Dynamic modelling of CO_2 absorption for post combustion capture in coal-fired power plants. Fuel 88 (12), 2455–2462.

Lepaumier, H., Picq, D., Carrette, P., 2009a. New amines for CO_2 capture. I. Mechanisms of amine degradation in the presence of CO_2. Industrial & Engineering Chemistry Research 48, 9061–9067.

Lepaumier, H., Picq, D., Carrette, P., 2009b. New amines for CO_2 capture. II. Oxidative degradation mechanisms. Industrial & Engineering Chemistry Research 48, 9068–9075.

Lepaumier, H., Martin, S., Picq, D., Delfort, B., Carrette, P., 2010. New amines for CO_2 capture. III. Effect of alkyl chain length between amine functions on polyamines degradation. Industrial & Engineering Chemistry Research 49, 4553–4560.

Liu, Y., Zhang, L., Watanasiri, S., 1999. Representing vapor–liquid equilibrium for an aqueous MEA-CO_2 system using the electrolyte nonrandom-two-liquid model. Industrial & Engineering Chemistry Research 38, 2080–2090.

Mccabe, W., Smith, J., Harriott, P., 2005. Unit Operations of Chemical Engineering, 7th ed. McGraw Hill Higher Education.

Mindrup, E.M., Schneider, W.F., 2010. Computational comparison of the reactions of substituted amines with CO_2. Chemistry and Sustainability ChemSusChem Energy and Materials 3, 931–938.

Onda, K., Takeuchi, H., Okumoto, Y., 1968. Mass transfer coefficients between gas and liquid phases in packed columns. Journal of Chemical Engineering of Japan 1, 52–56.

Oyenekan, B., 2007. Modeling of strippers for CO_2 capture by aqueous amines. Ph.D. dissertation, University of Texas at Austin.

Perry, R.H., Green, D.W., 1997. Perry's Chemical Engineers' Handbook, 7th ed. McGraw Hill.

Peng, D.Y., Robinson, D.B., 1976. A new two constant equation of state. Industrial Engineering Chemical Fundamentals 15, 59–64.

Qin, F., Wang, S., Hartono, A., Svendsen, H., Chen, C., 2010. Kinetics of CO_2 absorption in aqueous ammonia solution. International Journal of Greenhouse Gas Control 4, 729–738.

van Loo, S., van Elk, E.P., Versteeg, G.F., 2007. Removal of carbon dioxide with activated solutions of methyl-diethanol-amine. Journal of Petroleum Science and Engineering 55, 135–145.

Sexton, A.J., Rochelle, G.T., 2011. Reaction products from the oxidative degradation of monoethanolamine. Industrial & Engineering Chemistry Research 50, 667–673.

Simon, L., Yannick, E., Graeme, P., Artanto, Y., Hungerbuhler, K., 2011. Rate based modeling and validation of a carbon-dioxide pilot plant absorption column operating on monoethanolamine. Chemical Engineering Research and Design 89 (9), 1684–1692.

Taylor, R., Krishna, R., 1993. Multicomponent Mass Transfer. Wiley, New York.

-Tontiwachwuthikul, P., Meisen, A., Lim, C.J., 1992. CO_2 absorption by NaOH, monoethanolamine, and 2-amino-2-methyl-1-propanol solutions in a packed column. Chemical Engineering Science 47, 381–390.

Wilson, I., 2004. Gas liquid contact area of random and structured packing. M.S. thesis, University of Texas at Austin.

Zhang, Y., Chen, H., Chen, C., Plaza, J.M., Dugas, R., Rochelle, G.T., 2009. Rate-based process modeling study of CO_2 capture with aqueous monoethanolamine solution. Industrial & Engineering Chemistry Research 48, 9233–9246.